Multi-resolution MPS method for 2D free surface flows

Z.Y. Tang[1,2], Y.L. Zhang[1,2] and D.C. Wan[1,2]*

1. State Key Laboratory of Ocean Engineering, School of Naval Architecture, Ocean and Civil Engineering, Shanghai Jiao Tong University,
2. Collaborative Innovation Center for Advanced Ship and Deep-Sea Exploration, Shanghai 200240, China

*Corresponding author: dcwan@sjtu.edu.cn

Abstract

A multi-resolution MPS (Moving Particle Semi-implicit) method is applied into 2D free surface flows based on our in-house particle solver MLParticle-SJTU in the present work. The basic idea of the present MPS method is to distribute high-resolution particles in the local concern region and low-resolution particles in the other region, such that both the number of particles and the computational cost can be reduced without sacrificing the corresponding accuracy. Considering the effect of different size particles, the kernel function is modified for gradient and Laplacian models and the incompressible condition between different size particles is enforcing by increasing the weight of divergence of velocity in the mixed source term of PPE (Poisson Pressure Equation). In order to validate the present MPS method, two cases are carried out. Firstly, a hydrostatic case is performed. The results show that the contour of pressure field by multi-resolution MPS is quite agreement with that by single resolution MPS. Especially, the multi-resolution MPS can still provide a relative smooth pressure together with single resolution MPS in the vicinity of the interface between the high-resolution and low-resolution particles. For a long time simulation, the kinetic energy of particles by multi-resolution MPS can decrease quickly to the same level as that of single resolution MPS. In addition, a 2D dam breaking flow is simulated and the multi-resolution case can run stably during the whole simulation. The pressure by the multi-resolution MPS is in agreement with experimental data together with single resolution MPS. The contour of pressure field by the former is also similar to that by the later. In addition, the simulation by multi-resolution MPS is as accurate as the traditional MPS with fine particles distributed in the whole domain and the corresponding CPU time can be reduced.

Keywords: Multi-resolution method, MPS (Moving Particle Semi-Implicit), dam breaking, free surface flows

Introduction

In recent years, meshfree particle methods have been developed widely and applied successfully into practical engineering. Unlike the mesh-based method, the fluid is presented as a set of Lagrangian particles in the meshfree method and there is no constant topology relationship between these particles. Thanks to the Lagrangian nature, the particle method is very suitable to deal with flow with largely deformed free surface and moving boundaries [Liu (2008); Khayyer (2008); Tanaka (2010)]. MPS (Moving Particle Semi-implicit) is one of such meshfree methods, which is first proposed by Koshizuka [(1996; 1998)] and then improved by numerous MPS practitioners [Tanaka and Masunaga (2010); Khayyer and Gotoh (2012); Kondo and Koshizuka (2011); Zhang and Wan (2012a)]. Up to now, this method has been applied into a wide variety of violent free surface flows, such as liquid sloshing [Zhang and Wan (2012b; 2014)], dam breaking [Khayyer and Gotoh (2012); Shakibaeinia and Jin (2011)], wave breaking [Gotoh and Sakai (2006); Khayyer and Gotoh (2008); Tang et al. (2014)], green water [Zhang et al. (2013)] and ship-wave interaction [Shibata et al. (2012)]. Despite being an excellent method for solving the largely deformed free surface problems, it still suffers from high computational cost. Especially when applied into 3D simulations, a great number of particles are necessary and the required CPU time can increase sharply. To overcome this problem, multi-resolution simulation are introduced to accelerate the computation. In the framework of SPH, Vacondio et al. [(2012; 2013)] presented a dynamic particle refine algorithm based on particle merging and coalescing during the simulation. Omidvar et al. [(2013)] studied the wave body interaction using variable particle mass distribution. Most of these

works are carried out based on explicit algorithm. Unlike the SPH, the pressure field is obtained based on semi-implicit algorithm in the MPS method. The consuming time per one time level in the later method is much more than that in the former. Many MPS practitioners attempt to introduce the multi-resolution simulation in the MPS. Shibata et al. [(2012)] proposed an overlapping particle technique (OPT) and applied it into a 2D green water. Tanaka [(2009)] presented a multi-resolution method based on traditional MPS. Unfortunately, validation is not given in the article.

In the present work, the multi-resolution technique is applied into 2D free surface flows based on modified MPS [Zhang and Wan (2012a); Zhang et al. (2014)]. Considering the effect of different size particles, the kernel function is modified for gradient and Laplacian models. The incompressible condition between different size particles is enforcing by increasing the weight of divergence of velocity in mixed source term of PPE. In order to validate the present MPS method, two cases are carried out. Firstly, a hydrostatic case is performed. The pressure field and the kinetic energy for fluid particles by multi-resolution MPS are compared with that by single resolution MPS with fine particle distributed in the entire domain. In addition, a 2D dam breaking flow is simulated and the multi-resolution case can run stably during the whole simulation. The comparison among the pressure by single resolution MPS and multi-resolution MPS and experimental data is also made.

NUMERICAL SCHEME

Governing Equations

In the MPS method, governing equations are the mass and momentum conservation equations. They can read as:

$$\frac{1}{\rho}\frac{D\rho}{Dt} = -\nabla \cdot \boldsymbol{V} = 0 \tag{1}$$

$$\frac{D\boldsymbol{V}}{Dt} = -\frac{1}{\rho}\nabla P + \nu\nabla^2\boldsymbol{V} + \boldsymbol{g} \tag{2}$$

Where: ρ is the fluid density, $\boldsymbol{V}$ is the velocity vector, P presents the pressure, ν is the kinematic viscosity, and $\boldsymbol{g}$ is gravitational acceleration vector, t indicates the time. It is noted that Eq. (1) is only available for incompressible fluid.

Particle Interaction Models

Kernel Function

In the original MPS method, the kernel function (Eq. (3)) first proposed by Koshizuka [(1998)] is usually employed by MPS researchers. However, it has a drawback due to its singular at $r = 0$. Conversely, we adopt an improved kernel function introduced by Zhang [(2012a)]:

$$W(r) = \begin{cases} \dfrac{r_e}{r} - 1 & 0 \le r < r_e \\ 0 & r_e \le r \end{cases} \tag{3}$$

$$W(r) = \begin{cases} \dfrac{r_e}{0.85r + 0.15r_e} - 1 & 0 \le r < r_e \\ 0 & r_e \le r \end{cases} \tag{4}$$

Where r_e denotes the radius of the particle interaction. According to Koshizuka's suggestion, the radius adopted in particle number density and the gradient model is $r_e = 2.1l_0$, while $r_e = 4.01l_0$ is used for the Laplacian model, where l_0 is the initial distance between two adjacent particles.

Gradient Model

In MPS, the gradient operator is discretized as weighted average of the gradient vector between particles i and its neighboring particle j, it can be given as:

$$< \nabla P >_i = \frac{\mathrm{d}}{n^0} \sum_{j \neq i} \frac{P_j - P_i}{| \boldsymbol{r}_j - \boldsymbol{r}_i |^2} (\boldsymbol{r}_j - \boldsymbol{r}_i) \cdot W(| \boldsymbol{r}_j - \boldsymbol{r}_i |) \tag{5}$$

Eq. (5) cannot conserve the linear and angular momentum of the system, and a conservative form is introduced as following [Tanaka and Masunaga (2010)]:

$$< \nabla P >_i = \frac{\mathrm{d}}{n^0} \sum_{j \neq i} \frac{P_j + P_i}{| \boldsymbol{r}_j - \boldsymbol{r}_i |^2} (\boldsymbol{r}_j - \boldsymbol{r}_i) \cdot W(| \boldsymbol{r}_j - \boldsymbol{r}_i |) \tag{6}$$

Where n^0 is the initial particle number density, d indicates the number of space dimensions, $\boldsymbol{r}$ presents the coordinate vector of fluid particle.

Divergence Model

Similar to gradient model, the divergence model for vector $\boldsymbol{V}$ can be formulated as [Shakibaeinia and Jin (2012)]:

$$< \nabla \cdot \boldsymbol{V} >_i = \frac{\mathrm{d}}{n^0} \sum_{j \neq i} \frac{(\boldsymbol{V}_j - \boldsymbol{V}_i) \cdot (\boldsymbol{r}_j - \boldsymbol{r}_i)}{| \boldsymbol{r}_j - \boldsymbol{r}_i |^2} \boldsymbol{W}(| \boldsymbol{r}_j - \boldsymbol{r}_i |) \tag{7}$$

Laplacian Model

The Laplacian operator is modeled by weighted average of the distribution of a quantity ϕ from particle i to its neighboring particle j, it can read as the following equations:

$$< \nabla^2 \phi >_i = \frac{2\,\mathrm{d}}{n^0 \lambda} \sum_{j \neq i} (\phi_j - \phi_i) \cdot W(| \boldsymbol{r}_j - \boldsymbol{r}_i |) \tag{8}$$

$$\lambda = \frac{\sum_{j \neq i} W(| \boldsymbol{r}_j - \boldsymbol{r}_i |) \cdot | \boldsymbol{r}_j - \boldsymbol{r}_i |^2}{\sum_{j \neq i} W(| \boldsymbol{r}_j - \boldsymbol{r}_i |)} \tag{9}$$

Where, the parameter λ is introduced to keep the variance increase equal to the analytical solution.

Model of Incompressibility

In the MPS method, the incompressibility is assured by keeping the particle number density constant. There are two stages in each time step when incompressible condition is enforced: firstly, temporal velocity of particles is calculated explicitly under the action of viscous and gravitational forces, and particles move to intermediate location; secondly, pressure fields are obtained implicitly through solving the Poisson Pressure Equation (PPE), and the velocity and position of particles are updated based on the obtained pressure.

The Poisson Pressure Equation in MPS method is first derived by Koshizuka [(1998)] as following:

$$< \nabla^2 P^{k+1} >_i = \frac{\rho}{\Delta t^2} \frac{< n^* >_i - n^0}{n^0} \tag{10}$$

Where n^* is the intermediate particle number density, Δt denotes the calculation time step.

Eq. (10) is commonly employed by many MPS practitioners. However, the source term of the PPE only consists of the deviation of the temporal particle number density from the initial value, and this may lead to high oscillation pressure field in spatial and temporal domain because of unsmooth particle number density. To stabilize the pressure calculation, a mixed source term method combining the velocity divergence-free and constant particle number density is investigated by Tanaka et al. [(2010)] and rewritten by Lee et al. [(2011)] as:

$$< \nabla^2 P^{k+1} >_i = (1-\gamma) \frac{\rho}{\Delta t} \nabla \cdot V_i^* - \gamma \frac{\rho}{\Delta t^2} \frac{< n^k >_i - n^0}{n^0} \tag{11}$$

Where the subscript k and k +1 indicate the physical quantity in the k th and k +1 th time step, γ is the weight of the particle number density in the source term and is assigned a value between 0 and 1. In this paper, γ = 0.01 is selected.

Detection of Free Surface Particles

In the original MPS method, zero pressure boundary condition are enforced to the free surface particles. Free surface particles are recognized as the particle number density satisfying the following condition [Koshizuka (1998)]:

$$n_i^* < \beta \cdot n^0 \tag{12}$$

Where n^0 is the initial particle number density, and β indicates a threshold parameter and can be chosen between 0.8 and 0.99. However, misjudgment may occur for inner particles with small particle number density, and imposed unphysical false zero pressure may increase the oscillation frequency and amplitude of pressure field. To overcome this, some approaches have been developed to improve the accuracy of surface particle detection. Tanaka et al. [(2010)] judged the surface particle by using number of neighbor particles. This approach is further improved by Lee et al. [(2011)]. Khayyer et al. [(2009)] proposed a new criteria based on asymmetry of neighboring particles in which particles are judged as surface particles according to the summation of x-coordinate or y-coordinate of particle distance. In the present study, we employ a detection method [Zhang and wan (2012b)] which is also based on the asymmetry arrangement of neighboring

particles, but uses different equations, aiming at describing the asymmetry more accurately, as following:

$$\boldsymbol{F}_i = \frac{D}{n^0}\sum_{j\neq i}\frac{1}{\left|\boldsymbol{r}_i - \boldsymbol{r}_j\right|}\left(\boldsymbol{r}_i - \boldsymbol{r}_j\right)W\left(r_{ij}\right) \tag{13}$$

F is a vector with a large value near the free surface where the neighboring particles distribute largely asymmetry. In F function, the nearer neighboring particles have larger contribution, while further neighboring particles have smaller effect. This make F function not sensitive to the neighboring particles locating near the boundary of interaction domain.

If the absolute of the function $\boldsymbol{F}$ at particle i is more than a threshold α, then particle i is considered as free surface particle. Where α is assigned to $0.9|\boldsymbol{F}|^0$, $|\boldsymbol{F}|^0$ is the initial value of $|\boldsymbol{F}|$ for surface particle.

Modified Gradient and Laplacian Model

In the single resolution MPS, the interaction radius for each particle is the same as its neighbor particles. However, this condition cannot be ensured since both low-resolution particles with larger interaction radius and high-resolution particles with smaller interaction radius are distributed in the computational domain. This may lead to situations where two interaction particles i and j with different interaction radiuses. In the other words, the influence domain of particle i contains particles j but not vice versa. When calculating the force between particle i and its neighbor particle j, a violation of Newton's third law may occur. In the present work, the supported domain for two neighbor particles i and j is modified using the arithmetic mean. In particular, the cut-off radiuses for gradient and Laplacian models are presented as following respectively:

$$r_e = \left(r_{ei} + r_{ej}\right)\Big/2 \tag{14}$$

$$r_{e\_lap} = \left(r_{ei\_lap} + r_{ej\_lap}\right)\Big/2 \tag{15}$$

Define L is the particle diameter, the modification for gradient [Tanaka (2009)] and Laplacian models can be expressed as following:

$$\left\langle \nabla P\right\rangle_i = \frac{D}{n^0}\frac{P_j + P_i}{\left|\boldsymbol{r}_j - \boldsymbol{r}_i\right|^2}\left(\boldsymbol{r}_j - \boldsymbol{r}_i\right)W\left(\left|\boldsymbol{r}_j - \boldsymbol{r}_i\right|\right)\frac{L_j}{L_i} \tag{16}$$

$$\left\langle \nabla^2\phi\right\rangle_i = \frac{2D}{n^0}\left(\phi_j - \phi_i\right)W_{ij}\frac{\left(\frac{m_j}{L_i}\Big/\lambda_j + \frac{m_j}{L_j}\Big/\lambda_i\right)}{\frac{m_i}{L_i} + \frac{m_j}{L_j}} \tag{17}$$

TEST CASES

The hydrostatic case

In this section, the hydrostatic problem is carried out by the employment of the single resolution and multi-resolution MPS. A schematic view of the computational domain for this test is shown in

Fig. 1, where both the width of the water tank and the height of fluid are H = 1.0 m. The computational parameters are summarized in Table 1. In case A1, the entire computational domain is discretized by high resolution particles and the corresponding initial particle space is d = 0.01 m. In case A2, two kinds of particle size are employed where the yellow and blue regions are presented by high resolution (H/d=100) and low resolution (H/d=50) particles respectively. The height of the high resolution region in Case A2 is 0.4 m as the yellow region in Fig. 1. Specially note that the fact fluid height in Case A1 and A2 are 1.0 m and 0.995 m respectively.

Fig. 2 shows the pressure field after a long time evolution of the hydrostatic test. The contour of pressure field in the fine region by multi-resolution MPS is quite similar to that by single resolution MPS with fine particles. Furthermore, in the vicinity of the interface between the high and low resolution particles, a relative smooth pressure field can also be predicted by multi-resolution MPS.

Fig. 3 shows the comparison between the kinetic energy predicted by multi-resolution MPS and single resolution MPS, where the entire domain is represented by fine particles in the later, while the fine particles are only distributed in the yellow region in the former. In Fig. 3, the kinetic energy by multi-resolution MPS quickly decreases to the same level as that by single resolution MPS. This means that the disturbance produced in the interface between different particle sizes is not large, and can be reduced quickly as the initial disturbance in the uniform particle size simulation in this case.

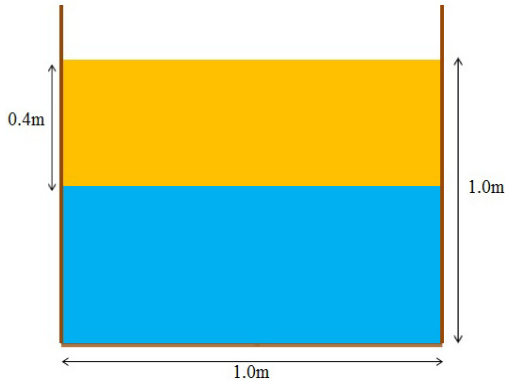

Figure 1. A schematic sketch of the computational domain for hydrostatic problem

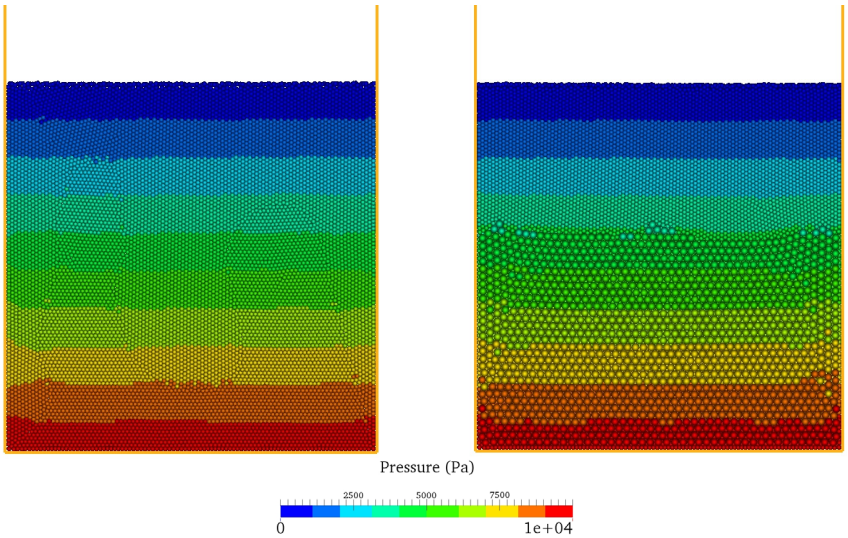

(a) Single resolution (b) Multi resolution

Figure 2. The pressure field predicted in Case A1 and A2

Table 1. Computational parameters in the simulations

Cases	Initial particle space (H/d)	Description
A1	100	Single resolution
A2	50，100	Multi resolution

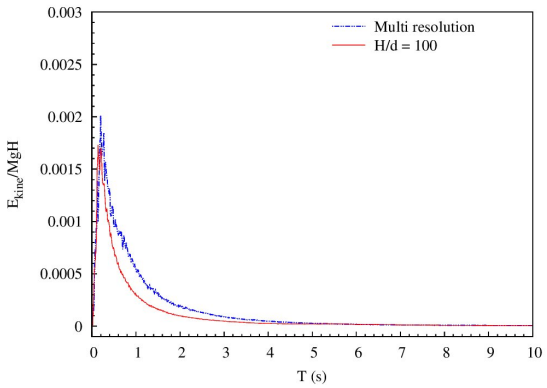

Figure 3. The comparison between the kinetic energy predicted by single resolution and multi-resolution MPS

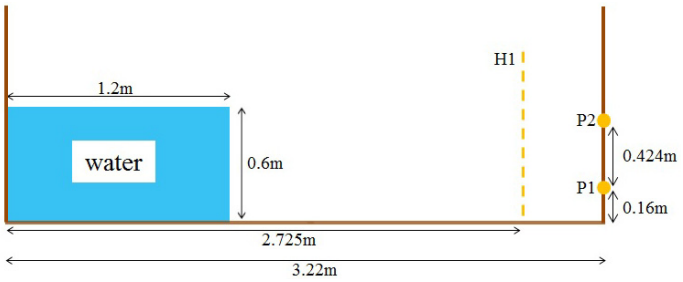

Figure 4. A schematic view of the computation domain for dam breaking

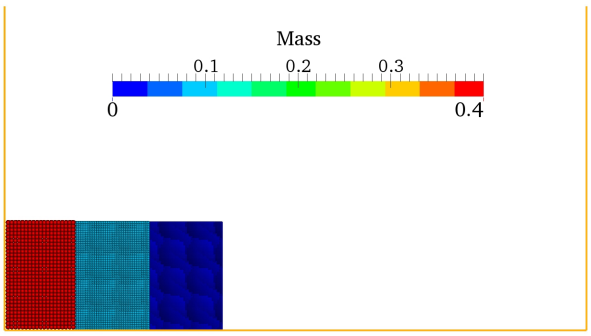

Figure 5. Initial particle mass distribution for 2D dam breaking problem

Dam Break Flow

Dam breaking is commonly computed as benchmark case for validation of CFD method in violent flows. In this paper, a dam break is simulated to verify the validation and efficiency of the Multi-resolution MPS method. A schematic view of the computational domain is shown in Fig. 4. The tank is 3.22 m long, 2.0 m high. Initial water column is 1.2 m long and 0.6 m high. The water is

initially constricted by a removable door which is picked up suddenly at $t = 0$ s. A wave height probe is placed at 2.725 m from the left boundary and two pressure probes are placed on the right wall. The initial particle mass distribution for multi-resolution simulation is depicted in Fig. 5, where three kinds of particle size are selected, including H/d=30, 60, 120, and corresponding masses are 0.4, 0.1 and 0.025 respectively.

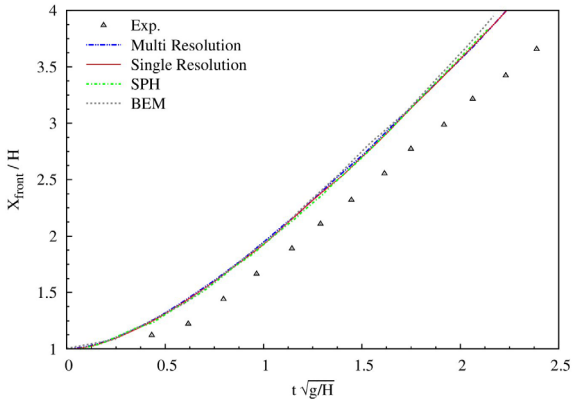

Figure 6. Propagation of the surge front after dam gate removal compared to literature data

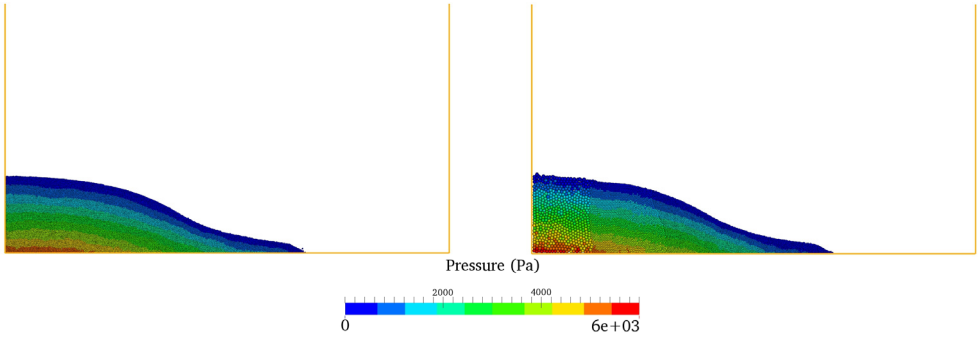

(a) Single resolution (b) Multi-resolution

Figure 7. Comparisons of dam-break flows using Single resolution and Multi-resolution MPS at $t\sqrt{g/H}$ =1.45

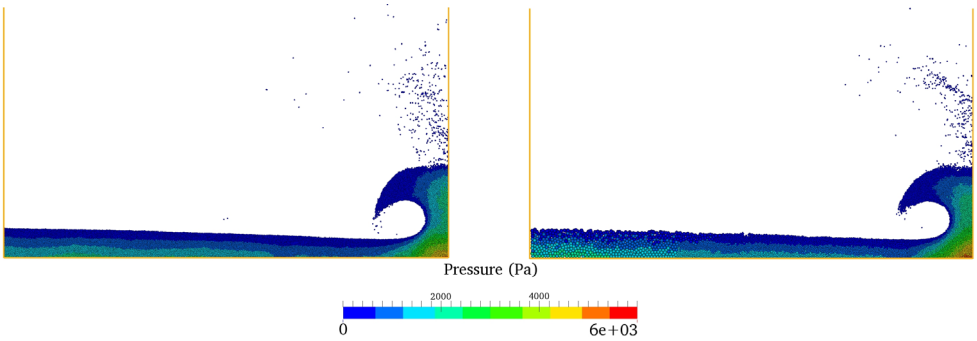

(a) Single resolution (b) Multi-resolution

Figure 8. Comparisons of dam-break flows using Single resolution and Multi-resolution MPS at $t\sqrt{g/H}$ =5.7

The wave front propagation along the downstream horizontal dry bed after the dam door release are shown in Fig. 6. The multi-resolution result is quite agreement with that of single resolution MPS and is also quite similar to that of SPH [Ferrari et al. (2009)] and BEM [Colagrossi and Landrini

(2003)]. However, the speed of the leading edge by these numerical results is quick than that of the experiment. Similar results can also be reported in literatures [Koshizuka and Oka (1996); Rogers et al. (2010); Abdolmaleki (2004)].

In Fig. 7 and Fig. 8, the pressure fields by single resolution and multi-resolution MPS are depicted for comparison. It can be seen that the computed pressure fields are both relative smooth throughout the time of flow propagation, free surface overturning and impacting the underline water. The contour of the pressure field by multi-resolution MPS is also similar to that by single resolution MPS.

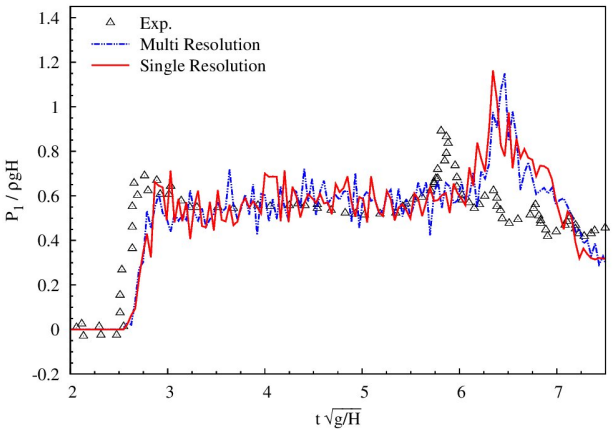

Figure 9. Time variations of dimensionless pressure at the bottom of the probe P1

The detailed comparisons of time variations of pressure results at the bottom of the probe P1 are shown in Fig. 9, it can be seen that the overall tendency of pressure variation by both the single resolution and multi-resolution MPS is quite in agreement with experimental data except a clear discrepancy between the position of second pressure peak by the numerical results and experimental data, which is also reported by many researchers employing the single phase model [Marrone et al. (2011); Khayyer et al. (2009)]. However, the pressure variation by multi-resolution MPS is quite close to that of single resolution MPS, including the first impact time and the position of the second pressure peak.

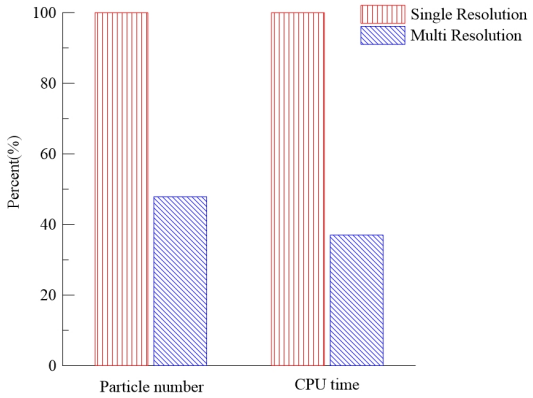

Figure 10. The number of particles and required CPU time for flowing 3 seconds

Fig. 10 shows the total number of particles and required CPU time for flowing 3s by conventional single resolution MPS and multi-resolution MPS. Both of these two cases are carried out on personal computer with Intel i7-3770. From the Fig. 10, the number of particles by multi-resolution MPS is nearly half of that by single resolution MPS, while the consuming CPU time in the later is

about two times and a half than that in the former. As presented by Koshizuka [(1988)], the consuming time for solving PPE is proportional to $N^{1.5}M^{0.5}$, where N is the number of particles and M presents the average number of neighboring particles. The number of particles in multi-resolution MPS is less than that in single resolution MPS, which means that multi-resolution MPS can reduce the number of particles and further decrease the required CPU time. Therefore, the multi-resolution method can be an alternative way to reduce the required computational time if one only concern the local region. Furthermore, considering the pressure variation and the contour of pressure field between single and multi-resolution MPS, the multi-resolution MPS can reduce the CPU time without sacrificing the accuracy.

Conclusions

In this paper, the multi-resolution MPS method is applied into 2D free surface flows based on in-house particle solver MLParticle-SJTU. In particular, the entire computation domain is discretized with both the low-resolution and high-resolution particles, where only the high-resolution particles are distributed in the concerned local region. Considering the effect of different size particles, the kernel function is modified for gradient and Laplacian models and the incompressible condition between different size particles is enforcing by increasing the weight of divergence of velocity in the mixed source term of PPE. To verify the availability and efficiency of the multi-resolution MPS, two cases are carried out. Firstly, a hydrostatic case is performed. The results show that the contour of pressure field by multi-resolution MPS is nearly the same as that of single resolution MPS. Especially, the multi-resolution MPS can still provide a relative smooth pressure in the vicinity of the interface between the high-resolution and low-resolution particles. For a long time simulation, the kinetic energy of particles by multi-resolution MPS can decrease quickly to the same level as that of single resolution MPS with fine particles distributed in the entire domain. In addition, a 2D dam break flow is carried out and the multi-resolution case can run stably during the whole simulation. Both the pressure variation at the measuring position and the contour of the pressure field at different times by multi-resolution MPS are quite in agreement with that of single resolution MPS. Considering the required CPU time of these two methods, multi-resolution MPS can reduce the computational time without sacrificing its accuracy.

From the above mentioned, it can be seen that the multi-resolution MPS can reduce the required number of particles and further decrease the computational cost. When the traditional MPS is applied into 3D free surface flows such as ship-wave interaction, a great number of particles are necessary and the computational cost can increase sharply. The multi-resolution MPS can be an alternative method to solve this problem and relative work is ongoing.

Acknowledgement

This work is supported by National Natural Science Foundation of China (Grant Nos. 51379125, 51490675, 11432009, 51411130131), The National Key Basic Research Development Plan (973 Plan) Project of China (Grant No. 2013CB036103), High Technology of Marine Research Project of The Ministry of Industry and Information Technology of China, Chang Jiang Scholars Program (Grant No. T2014099) and the Program for Professor of Special Appointment (Eastern Scholar) at Shanghai Institutions of Higher Learning (Grant No. 2013022), to which the authors are most grateful.

References

Abdolmaleki, K., Thiagarajian, K. P. and Morris-Thomas, M. T. (2004) *Simulation of the dam break problem and impact flows using a Navier-Stokes solver*, Proc 15th Australasian Fluid Mechanics Conference, Sydney.

Colagrossi, A., and Landrini, M. (2003) Numerical simulation of interfacial flows by smoothed particle hydrodynamics, Journal of Computational Physics **191**, 448-475.

Ferrari, A., Dumbser, M., Toro, E. F., and Armanini, A. (2009) A new 3D parallel SPH scheme for free surface flows, *Computers and Fluids* **38**, 1203-1217.

Gotoh, H., and Sakai, T. (2006) Key issues in the particle method for computation of wave breaking, *Coastal Engineering* **53**, 171-179.

Hori, C., Gotoh, H., Ikari, H., and Khayyer, A. (2011) GPU-acceleration for moving particle semi-implicit method. *Computers and Fluids* **51**, 174-183.

Khayyer, A., and Gotoh, H. (2008) Development of CMPS method for accurate water-surface tracking in breaking waves, *Coastal Engineering Journal* **50**, 179-207.

Khayyer, A., Gotoh, H., and Shao, S. D. (2008) Corrected incompressible SPH method for accurate water-surface tracking in breaking waves, *Coastal Engineering* **55**, 236-250.

Khayyer, A., Gotoh, H., and Shao, S. (2009) Enhanced predictions of wave impact pressure by improved incompressible SPH methods, *Applied Ocean Research* **31**, 111-131.

Khayyer, A., and Gotoh, H. (2012) A 3D higher order Laplacian model for enhancement and stabilization of pressure calculation in 3D MPS-based simulations, *Applied Ocean Research* **37**, 120-126.

Kondo, M., and Koshizuka, S. (2011) Improvement of stability in moving particle semi‐implicit method, *International Journal for Numerical Methods in Fluids* **65**, 638-654.

Koshizuka, S., Nobe, A., and Oka, Y. (1998) Numerical analysis of breaking waves using the moving particle semi-implicit method, *International Journal for Numerical Methods in Fluids* **26**, 751-769.

Koshizuka, S., and Oka, Y. (1996) Moving-particle semi-implicit method for fragmentation of incompressible fluid, *Nuclear science and engineering* **123**, 421-434.

Lee, B. H., Park, J. C., Kim, M. H., and Hwang, S. C. (2011) Step-by-step improvement of MPS method in simulating violent free-surface motions and impact-loads, *Computer methods in applied mechanics and engineering* **200**, 1113-1125.

Liu, M. B., Liu, G. R., and Zong, Z. (2008) An overview on smoothed particle hydrodynamics, *International Journal of Computational Methods* **5**, 135-188.

Marrone, S., Antuono, M., Colagrossi, A., Colicchio, G., Touzé, D. L., and Graziani, G. (2011) δ-SPH model for simulating violent impact flows, *Computer Methods in Applied Mechanics and Engineerin*g **200**, 1526-1542.

Omidvar, P., Stansby, P. K., and Rogers, B. D. (2013) SPH for 3D floating bodies using variable mass particle distribution, *International Journal for Numerical Methods in Fluids* **72**, 427-452.

Rogers, B. D., Dalrymple, R. A., and Crespo, A. J. C. (2010) State of the art of classical SPH for free surface flows, *Journal of Hydraulic Research* **48**, 6-27.

Shakibaeinia, A., and Jin, Y. C. (2011). A mesh-free particle model for simulation of mobile-bed dam break, *Advances in Water Resources* **34**, 794-807.

Shakibaeinia, A., and Jin, Y. C. (2012) MPS mesh-free particle method for multiphase flows, *Computer Methods in Applied Mechanics and Engineering* **229**, 13-26.

Shibata, K., Koshizuka, S., Sakai, M., and Tanizawa, K. (2012) Lagrangian simulations of ship-wave interactions in rough seas, *Ocean Engineering* **42**, 13-25.

Shibata, K., Koshizuka, S., and Tamai, T. (2012). *Overlapping particle technique and application to green water on deck,* Proceedings of 2nd International Conference on Violent Flows, Nantes, France.

Tanaka, M., and Masunaga, T. (2010) Stabilization and smoothing of pressure in MPS method by quasi-compressibility, *Journal of Computational Physics* **229**, 4279-4290.

Tanaka, M., Masunaga, T., and Nakagawa Y. (2009) Multi-resolution MPS method, *Transactions of JSCES*.

Tang, Z. Y., Zhang, Y. X., Li, H. Z., and Wan, D. C. (2014) *Overlapping MPS method for 2D free surface flows*, Proceedings of the 24th International Ocean and Polar Engineering Conference, Busan.

Vacondio, R., Rogers, B. D., and Stansby, P. K. (2012) Accurate particle splitting for smoothed particle hydrodynamics in shallow water with shock capturing, *International Journal for Numerical Methods in Fluids* **69**, 1377-1410.

Vacondio, R., Rogers, B. D., Stansby, P. K., Mignosa, P., and Feldman, J. (2013) Variable resolution for SPH: a dynamic particle coalescing and splitting scheme, *Computer Methods in Applied Mechanics and Engineering* **256**, 132-148.

Zhang, Y. X., and Wan, D. C. (2012a) Numerical Simulation of liquid sloshing in low-filling tank by MPS, *Chinese Journal of Hydrodynamics* **27**, 100-107.

Zhang, Y. X., and Wan, D. C. (2012b) *Apply MPS method to simulate liquid sloshing in LNG tank,* In Proceedings of the 22nd international offshore and polar engineering conference , Rhodes.

Zhang, Y. X., and Wan, D. C. (2014) Comparative study of MPS method and level-set method for sloshing flows, *Journal of Hydrodynamics* **26**, 577-585.

Zhang, Y. X., Wang, X., Tang, Z. Y., and Wan, D. C. (2013) *Numerical Simulation of Green Water Incidents Based on Parallel MPS Method,* In The Twenty-third International Offshore and Polar Engineering Conference, International Society of Offshore and Polar Engineers, Alaska.

Zhang Y. X., Yang Y. Q., Tang Z. Y., and Wan D. C. (2014) *Parallel MPS method for Three-Dimensional liquid sloshing*, Proceedings of the 24th International Ocean and Polar Engineering Conference, Busan.

Zhu, X., Cheng, L., Lu, L., and Teng, B. (2011) Implementation of the moving particle semi-implicit method on GPU, *Science China Physics, Mechanics and Astronomy* **54**, 523-532.